The Towing Mode, a spectroscopic tool for nuclear structure

V. Lima, J.A. Scarpaci, Y. Blumenfeld, C. Bourgeois, M. Chabot, P. Chomaz, P. Desesquelles, Valentin Duflot, J. Duprat, Muriel Fallot, et al.

HAL Id: in2p3-00021813

https://hal.in2p3.fr/in2p3-00021813

Submitted on 19 Jul 2004

The Towing Mode, a spectroscopic tool for nuclear structure

V.Lima [a], J.A.Scarpaci [a], Y.Blumenfeld [a], C.Bourgeois [a], M.Chabot [a],
Ph.Chomaz [b], P.Desesquelles [a], V.Duflot [b], J.Duprat [a], M.Fallot [a],
N.Frascaria [a], S.Grévy [c], D.Guillemaud-Mueller [a], D.Lacroix [c],
J.Margueron [b], P.Roussel-Chomaz [b], H.Savajols [b], O.Sorlin [a]

[a] *Institut de Physique Nucléaire d'Orsay, IN2P3-CNRS, Orsay, France*
[b] *GANIL, DSM-CEA/IN2P3-CNRS, Caen, France*
[c] *Laboratoire de Physique Corpusculaire (LPC), IN2P3-CNRS, Caen, France*

Abstract

The one-neutron halo ^{11}Be nucleus ground state has been studied using the ^{11}Be(^{48}Ti, ^{10}Be + n + γ) breakup reaction at 41 MeV/u at the GANIL facility. Experimental neutron energy distributions in coincidence with the ^{10}Be, with and without γ rays, have been extracted and compared to the calculated neutron energy distributions obtained with a time-dependent Schrödinger equation calculation for 2s, 1d and 1p wave functions. The comparisons between the data and the calculations lead to spectroscopic factors.

1   Introduction

The improvement of radioactive beam quality provides the opportunity to study nuclei with very exotic properties. The discovery of the halo nuclei at the end of the last century prompted new questions regarding the behaviour of nuclear structure far from stability. Since the discovery of its one-neutron halo configuration, ^{11}Be has been studied in several experiments. Indeed, the small separation energy (506 ± 4 kev [1]) and the low angular momentum value of the valence neutron lead to a very extended wave function; consequently, the picture of a two body system (n+core) is commonly used to describe this nucleus [2, 3]. Moreover, the structure of the ^{11}Be ground state presents a "parity inversion" between the $1/2^+$ and the $1/2^-$ neutron orbitals; several theoretical approaches [4, 5, 6, 7] showed the need for including the 2^+ excited state of the ^{10}Be core to reproduce this level inversion. The contribution from 2^+ ^{10}Be excitations in the ground state of ^{11}Be was studied in two recent experiments [8, 9]. The transfer reaction ^{11}Be(p, d)^{10}Be study of S. Fortier *et al.* and the breakup reaction ^{11}Be(^{9}Be, ^{10}Be+γ) experiment of T. Aumann *et al.* have deduced that the ground state of ^{11}Be has 80% contribution from the $s_{1/2} \otimes ^{10}$Be(0^+) configuration and 20% from the $d_{5/2} \otimes ^{10}$Be(2^+) configuration.
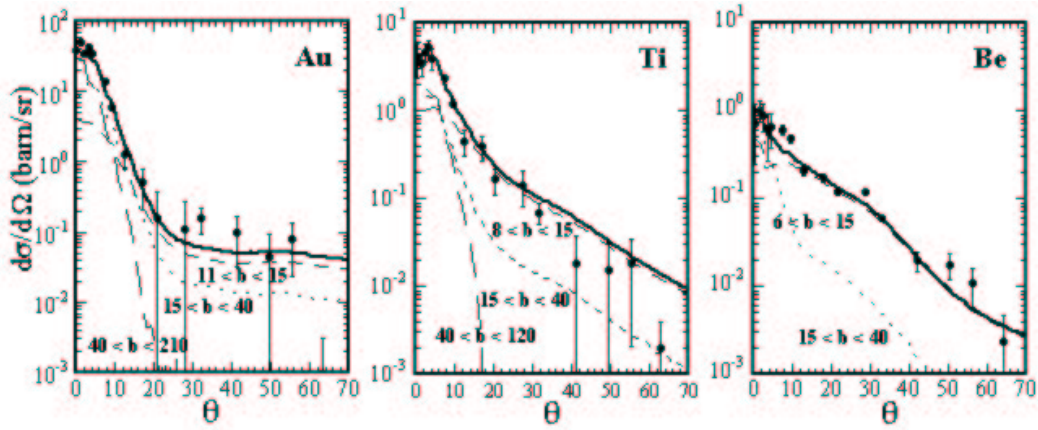
Figure 1: *Experimental neutron angular distributions from the $^{11}Be(^9Be$, ^{48}Ti and ^{197}Au, ^{10}Be +n) reaction [10]. The data are compared with TDSE calculations for a 2s wave function bound by 500 keV (black curve). The dashed, dotted and long dashed curves are the contribution of the calculation of three impact parameter regions: $b < 15$ fm, $15 < b < 40$ fm and $b > 40$ fm, respectively. The Figure has been taken from [11].*

In 1994, R. Anne *et al.* measured the angular distribution in the laboratory frame of the neutron due to the breakup of ^{11}Be on ^{9}Be, ^{48}Ti and ^{197}Au targets at 41 MeV per nucleon [10]. The comparison between the data and a calculation using the eikonal approximation led them to conclude that the coulomb interaction was responsible for forward-angle neutron emission (less than 20°). The backward-angle portion of the neutron angular distribution was speculated to result from nuclear processes, though few details were provided in support of this claim. In 2001, M. Fallot *et al.* [11] compared the results from the latter experiment with a calculation derived from solving the time-dependent Schrödinger equation (TDSE) for a one body neutron wave function in dynamic potentials [12]. The comparison, presented here in Figure 1 for each target nucleus, shows excellent agreement in every case. As described in the figure, the calculation has been subdivided into contributions from three impact parameter bins: b less than 15 fm, b between 15 and 40 fm and b greater than 40 fm. For high impact parameter values (b > 40 fm), when the nuclear potential of the target does not interact with the wave function, the calculation predicts a neutron emission at forward angles. For low impact parameters (b < 15 fm), when the wave function interacts with the nuclear potential of the target, the calculation clearly reproduces the large-angle part of the neutron angular distribution. The reaction mechanism responsible for these large-angle neutron emissions has been previously described in the context of the results from a recent study of ^{40}Ar-induced ^{58}Ni breakup performed by J. A. Scarpaci et al. [13]. This mechanism, called the Towing Mode, is a generic phenomenon in the inelastic channel and occurs in peripheral collisions at intermediate energies: this is a *gentle* mechanism which leaves the target in a one-hole configuration when the nucleon is *towed* away by the projectile (or vice versa).

2

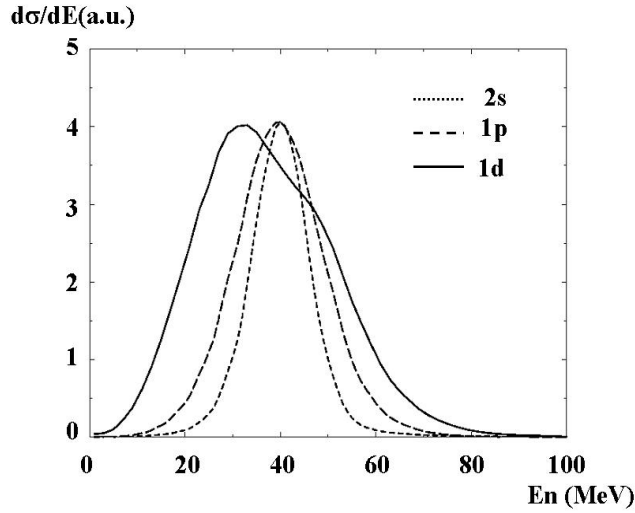Using this calculation, we have extracted the neutron energy distributions for

Figure 2: *Neutron energy distributions extracted from the TDSE calculation for 2s, 1p and 1d wave functions bound by 500 keV.*

large-angle neutron emission ($\theta > 20°$) for neutrons initially in the 2s, 1p and 1d wave functions bound by 500 keV in a ^{10}Be spherical Wood-Saxon potential and perturbed by a ^{48}Ti potential. The calculation predicts different shapes for the neutron energy distributions for the different angular momentum values (see Figure 2). Therefore, it seems possible to extract nuclear structure information using the comparison between experimental and calculated neutron energy distributions from these large angle emitted neutrons. Given that the calculations assumes 100% of an initial wave function, the normalization factor then needed to adjust the calculation to the data is directly related to the spectroscopic factor. In this way, the Towing Mode might be considered a candidate for spectroscopic studies. In order to test this idea we have performed a new ^{11}Be breakup measurement on ^{48}Ti target, aimed at enhancing the statistics for large-angle neutron emission. Additionally, a γ-ray detection system was incorporated so as to have the capability of discriminating between the excited states in the ^{10}Be core following neutron emission.

2 Experimental set-up

The experiment was performed at the GANIL facility (Caen, France) where a secondary beam of 8.10^4 ^{11}Be per second at 41 MeV per nucleon was produced by fragmentation of a ^{13}C primary beam in a 6120 μm ^{12}C target in the SISSI device. The ^{11}Be secondary beam was selected and purified in the α spectrometer with a 600 μm ^{26}Al degrader placed in the intermediate focal plane. A "parallel optic on target" beam line tune was required for this experiment. This tune provided a low angular divergence beam ($\pm 0.2°$) to the detriment of the intensity (8.10^4 instead of the 3.10^5 ^{11}Be per second previously provided
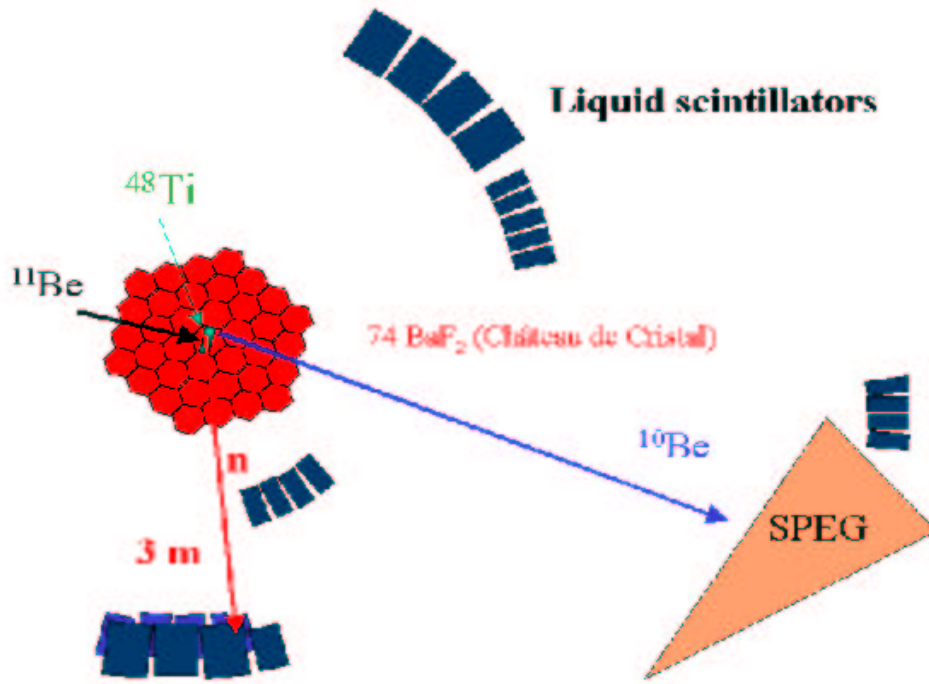
Figure 3: *Schematic view of the experimental set-up: 74 BaF$_2$ elements of the Château de Cristal array for the measurement of the γ rays, 30 liquid scintillators for the neutron detection and the SPEG spectrometer for ^{10}Be identification.*

by the GANIL). The ^{11}Be beam impinged on a 115 mg/cm^2 ^{48}Ti target placed in the SPEG experimental vault. The experimental set-up is presented in the figure 3.

The target was surrounded by 74 BaF$_2$ elements of the Château de Cristal array [14] to measure the γ ray coming from the decay of ^{10}Be excited states. The identification of particles was made by the time-of-flight method. 30 BC501 liquid scintillator detectors were arranged between 3° and 95° to measure the neutrons. The identification of detected particules was realised by pulse shape analysis and their energies were obtained from the time-of-flight of the particles. The ^{10}Be ejectile was identified in the focal plane of the SPEG spectrometer [15] positionned at zero degrees with respect to the beam direction and covering a laboratory frame scattering angle between -2.5° and +2.5°. Its standard detection system (2 drift chambers, 1 ionisation chamber and a plastic scintillator) also permitted a momentum determination for ejectiles.

3   Neutron angular distribution

Figure 4 presents the experimental angular distribution of the neutrons coming from the breakup of ^{11}Be under the same conditions as [10](black dots): energy neutron greather than 26 MeV and detected in coincidence with the ^{10}Be. Also shown are the experimental angular distribution from the previous study [10]
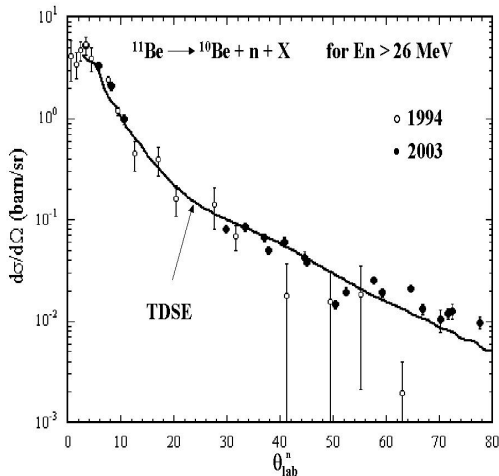
4

Figure 4: *Neutron angular distribution obtained in this experiment (black dots) compared with the previous data from the experiment [10] (open circles) and the time-dependent Schrödinger equation (TDSE) calculation for a 2s wave function (black curve).*

(open circles) and the calculated angular distribution (TDSE) for a 2s wave function (black line). Better statistics in the large angle region were obtained and the calculation is in very good agreement with the data over three orders of magnitude in differential cross section. In the following, we will focus on the study of the neutron energy distributions in coincidence with the ^{10}Be nucleus, with and without γ ray coincidence.

4 Study of the neutron energy distributions

Figure 5 presents the neutron energy distribution extracted in coincidence with ^{10}Be for neutrons detected at forward angles (a) and for neutrons detected at angles larger than 30° (b). Panels c and d present the same neutron energy distributions in coincidence with γ rays of energy greater than 1 MeV. The cut-off was determined to eliminate as much as possible the 980 kev energy γ ray contribution corresponding to the $2^+ \to 0^+$ decay of the ^{48}Ti target.

The energy distribution 5a is characterized by a peak centered around 40 MeV which is the energy per nucleon of the beam: these neutrons come from the coulomb breakup of ^{11}Be. Figure 5b is similar but displays a low energy component due to the emission of the target. When a γ ray is required, very few of the forward-peaked neutrons remain, as shown in Figure 5c. However, the γ-ray coincidence requirement on the large-angle neutron cut (Figure 5d) clearly shows the emergence of a peak near 25 MeV; again one observes the low energy contribution that results from target emission. Note that the low energy contribution does not appear in the forward spectra (a) and (c) due to the fact that the four neutron detectors placed between 3° and 10° were positioned behind the dipoles of the SPEG spectrometer, the low enery neutrons were absorbed before reaching the detectors.
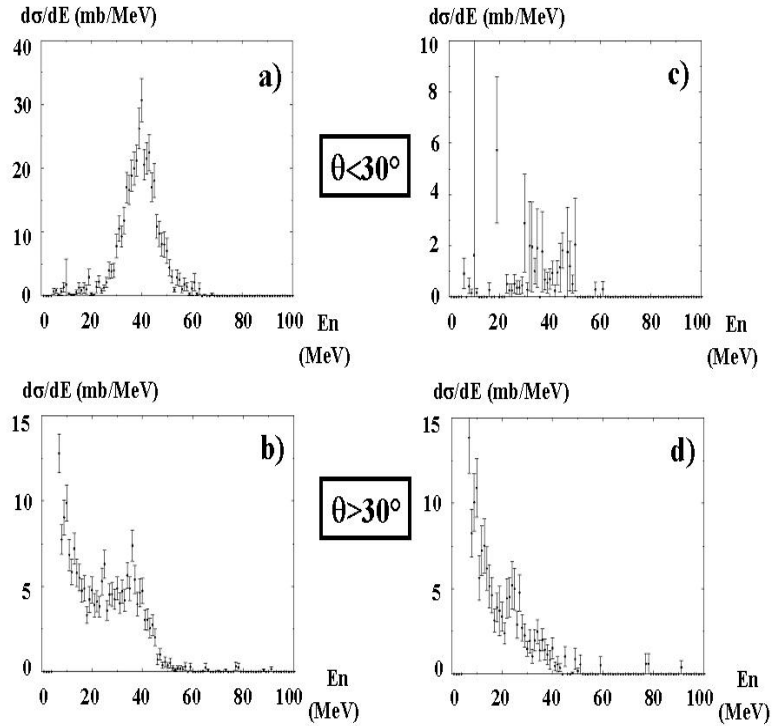
5

Figure 5: *Neutron energy distributions. a) and b) are extracted in coincidence with 10Be: a) for neutrons detected at forward angles, b) for neutron angles > 30°. c) and d) are distributions extracted in coincidence with the ^{10}Be and the γ rays: c) for neutrons detected at forward angles, d) for neutron angles > 30°.*

As discussed previously, nuclear structure information can be extracted by analysing the energy distributions of neutrons detected at large angles. We have focused our study on the $30° < \theta_n < 50°$ angle region for which the ratio, $\frac{signal}{noise}$, is optimal (the noise comes from the emission of the target).

5 Extraction of spectroscopic factors

5.1 No γ-ray emission

The first step of our work was to determine the neutron energy distribution when no γ ray was emitted. For this, we subtracted the neutron energy distribution detected in coincidence with ^{10}Be and a γ ray (corrected for the efficiency of detecting a γ ray of an energy higher than 1 MeV coming from the decay of the ^{10}Be excited states), Figure 6b, from the experimental spectrum of the inclusive channel, Figure 6a. The result is presented in Figure 6c and compared with the calculated energy distributions for 2s, 1d and 1p wave functions arbitrarily normalized to the data. The 1p wave function shown was calculated with a binding energy of 6.7 MeV to simulate the 1p neutron wave function of the ^{10}Be core. This subtracted data presents a peak centered
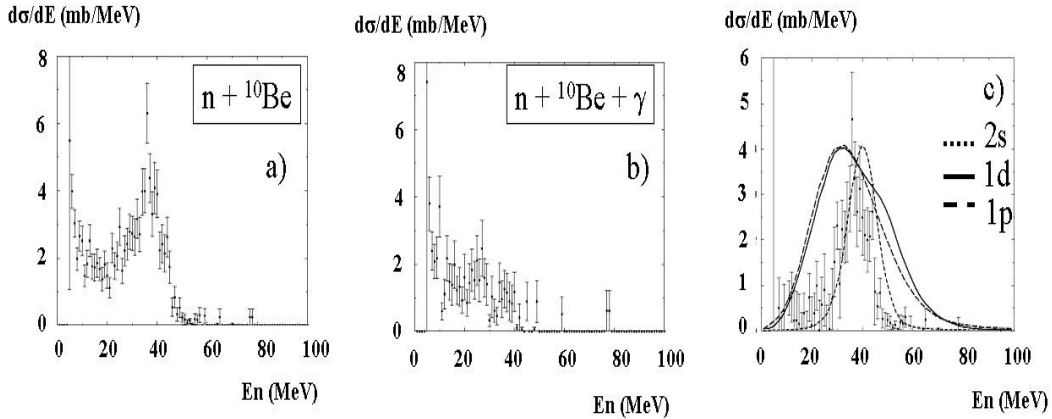
Figure 6: *Neutron energy distributions measured between* $30° < \theta_n < 50°$. *a) is the neutron distribution extracted in coincidence with the* ^{10}Be, *b) was extracted in coincidence with the* ^{10}Be *and the* γ *rays and c) shows the result of the subtraction (a) - (b). The spectrum c is compared with the calculated energy distribution for 2s, 1d and a 1p wave functions (with binding energy of 500, 500 and 6700 keV, respectively).*

around 37 MeV; the 2s shape of the energy distribution is more consistent with the data than those of the 1d and 1p energy distributions, even though it is slightly shifted. This result is in good agreement with previous studies [8, 9] that have described the $s_{1/2} \otimes ^{10}Be$(g.s.) contribution to the ^{11}Be ground state. The coefficient needed to adjust the calculation on the data is directly the value of the spectroscopic factor. The normalisation of the calculation on the data leads to a spectroscopic factor of S_{2s}=0.47±0.04 where the uncertainty quoted is purely statistical.

5.2 γ-ray emission required

We focus on the treatment of the neutron energy distribution measured in coincidence with the γ rays in the region $30° < \theta_n < 50°$. The spectrum is reported on figure 7 where the data has been condensed to 2 MeV per channel. To remove the contribution at low energies due to the emission of the target we first extracted the experimental spectrum of the neutrons measured in coincidence with the γ rays and ^{11}Be projectiles in SPEG. Neutrons in this channel result uniquely from target emission. This experimental neutron distribution, aribitrarily normalized, (Figure 7b) was subtracted from the distribution of neutrons in coincidence with ^{10}Be and γ rays. The result of the subtraction is shown in Figure 7c where it is compared to the three calculated energy distributions for the 2s, the 1d and the 1p wave functions. The shapes of the 1p and 1d neutron energy distributions agree equally well with the experimental results, thus confirming the expectation that no 2s neutrons should be seen in coincidence with ^{10}Be core excitations. Clearly, what remains to be quantified are the 1p and 1d contributions to the observed neutron energy distribution which can be extracted from the study of the γ-ray energy distribution.
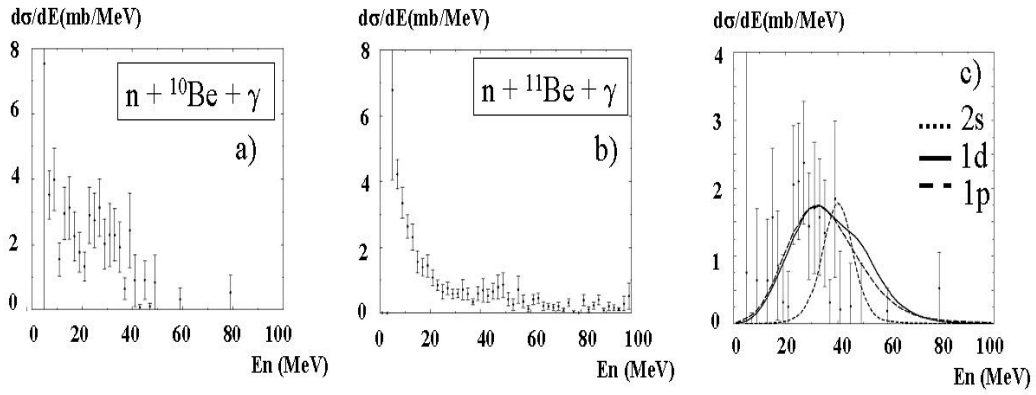
Figure 7: *Neutron energy distributions: a) in coincidence with the ^{10}Be, b) is in coincidence with the ^{11}Be (contribution of the target) and c) is the subtracted spectrum (a)-(b).*

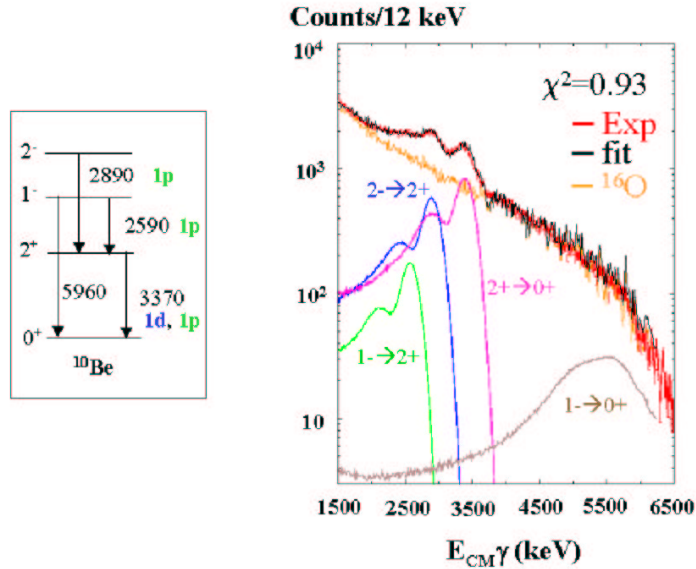### 5.2.1 GEANT simulation for the determination of the p and d neutron state contributions

Figure 8: *On the left, a partial level scheme of the ^{10}Be taken from [16]. On the right, the experimental γ-ray energy spectrum measured with the Château de Cristal array in coincidence with the ^{10}Be. The contributions of the $1^- \rightarrow 2^+$, $2^- \rightarrow 2^+$, $2^+ \rightarrow 0^+$ and $1^- \rightarrow 0^+$ transitions simulated by GEANT and the experimental background are also shown. The fit of the experimental data with these five components was performed by a χ^2 minimisation method and $\chi^2 = 0.93$ was found.*

The spectrum on figure 8 presents the experimental γ-ray energy distribution measured in coincidence with the ^{10}Be. Four main peaks coming from the decay of ^{10}Be excited states have been considered: the $1^- \rightarrow 2^+$, the $2^- \rightarrow 2^+$,

8

the $2^+ \rightarrow 0^+$ and the $1^- \rightarrow 0^+$ transitions characterised respectively by the emission of 2.59 MeV, 2.89 MeV, 3.37 MeV and 5.96 MeV γ rays, according to the partial level scheme [16] showed in the left panel of Figure 8. The 2^- and 1^- states are resulting from an one hole configuration in the $1p_{3/2}$ neutron subshell of the ^{11}Be and decay through the 2^+ excited state. The breakup of a 1d state neutron leaves the ^{10}Be in a 2^+ excited state characterised by the emission of a 3.37 MeV γ ray. This γ ray either comes from the emission of the 1d neutron or the 1p neutron. To quantify the proportion of d to p neutron emission, we have to know the contribution of each γ ray component in the experimental spectrum.

We used the 3.21 version of GEANT [17] to simulate the response of the 74 detectors of the Château de Cristal array (the simulation takes into account the velocity of the source). The experimental background was taken from the ^{18}O(^{48}Ti, ^{16}O + γ) reaction. We choose the experimental γ-ray spectrum of this reaction channel because of the low probability of exciting the doubly magic ^{16}O nucleus. The background γ-ray energy distribution does not display any peak.

A χ^2 minimization method was used to adjust the sum of the five contributions to best fit the experimental data. The adjusted contributions are presented in figure 8 where a $\chi^2 = 0.93$ value has been obtained. With the coefficients, we are able to measure the probability for leaving the ^{10}Be nucleus in the 1^-, 2^- or 2^+ states and, therefore, the probability of towing a p neutron or a d neutron. If we denote N_{1-}, N_{2-} and N_{2+}, the probabilities for leaving the ^{10}Be core in the 1^-, 2^- and 2^+ excited states, respectively and N_d and N_p the probabilities for emitting d and a p-shell neutrons from ^{11}Be, respectively, we have the following relations:

$$N_{2+} = N_d + N_p$$

and

$$N_p = N_{1-} + N_{2-}.$$

From the analysis of the data, we obtain $N_p/N_d = 2$, $i.e.$, the probability of towing a p-state neutron is twice the probability of towing a d-state neutron.

5.2.2 Spectroscopic factors for the p and the d states

Given the above concerning N_p/N_d and considering that the calculation predicts almost the same shapes for the p and d neutron energy distribution, we can conclude that 2/3 of the total contributions to figure 7c are due to p-state neutron contributions while the remaining 1/3 results from d-state neutron contributions. The comparison between the calculation and the data gives the following spectroscopic factors for the $1p_{3/2}$ and the $1d_{5/2}$ states: S_{1d}=0.44±0.09 and S_{1p}=4.2±1.0 have been obtained after normalization the calculation on the data. The relevent spectra are reported in Figure 9.

6 conclusion

We have reported the analysis made on the ^{11}Be(^{48}Ti, ^{10}Be + n + γ) reaction at 41 MeV per nucleon. Large angle neutron energy distribution in coincidence
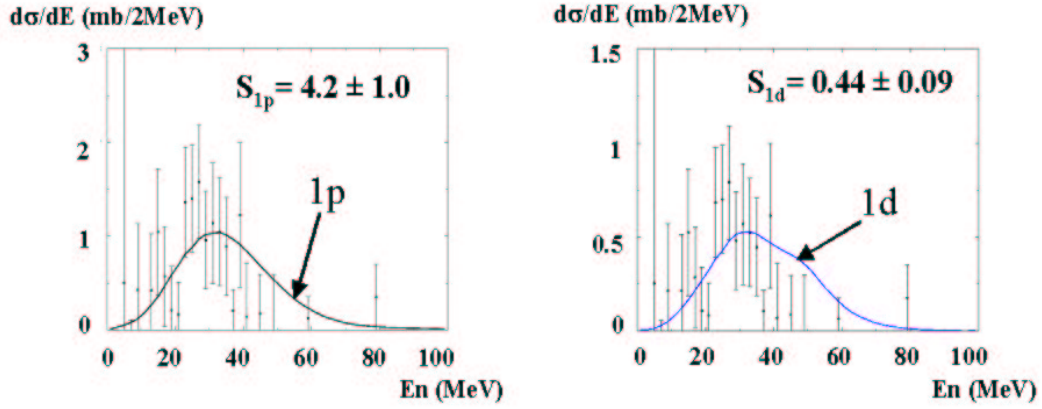
Figure 9: *On the left, Figure 7c multiplied by 2/3 and compared with the neutron energy distribution for a 1p wave function bound by 6.7 MeV. On the right, Figure 7c multiplied by 1/3 and compared with the neutron energy distribution for a 1d wave function bound by 500 keV. The spectroscopic factor S_{1p}=4.2±1.0 and S_{1d}=0.44±0.09 are obtained by scaling the calculated curves on the data.*

with the ^{10}Be with and without γ rays have been extracted and compared with results from time-dependent Schrödinger equation calculation. The following spectroscopic factors have been obtained: S_{2s}=0.47±0.04, S_{1p}=4.2±1.0 and S_{1d}=0.44±0.09. These values can be interpreted as the probability of occupation of the $2s_{1/2}$, $1p_{3/2}$ or $1d_{5/2}$ subshells. The reasonable values we obtain ($S_{2s} + S_{1d}$ close to 1 and the S_{1p} in a good agreement with the shell model for four neutrons in $1p_{3/2}$ subshell) are encouraging and challenge us to continue to develop this method. The measurement of spectroscopic factors is very sensitive to the accuracy of the data and the theoretical calculations. Further work on refining the calculation has to be done, *e.g.*, with the inclusion of the deformation of the ^{10}Be core. Nevertheless, the simple analysis of the energy distribution of the large angle emitted neutrons presents the Towing Mode process to be an interesting tool to study the structure of nuclei.

References

[1] J.H.Kelley *et al. Phys. Rev. Lett.*, 74:30, 1994.

[2] D.J.Millener *et al. Phys Rev C*, 28:497, 1983.

[3] P.G.Hansen. *Phys. Rev. Lett.*, 77:1016, 1996.

[4] B.A. Brown E.K. Warburton. *Phys. Rev. C*, 46:923, 1992.

[5] T.Otsuka. *Phys. Rev. Lett.*, 70:1385, 1993.

[6] P.Descouvemont. *Nucl. Phys. A*, 615:261, 1997.

[7] N.Vinh-Mau. *Nucl. Phys. A*, 592:33, 1995.

[8] S.Fortier *et al. Phys. Lett. B*, 461:22, 1999.

[9] T.Aumann *et al. Phys. Rev. Lett.*, 84:35, 2000.

[10] R.Anne *et al. Nucl. Phys. A*, 575:125, 1994.

[11] M.Fallot *et al. Nucl. Phys. A*, 700:70, 2002.

[12] D.Lacroix *et al. Nucl. Phys. A*, 658:273, 1999.

[13] J.A.Scarpaci *et al. Phys. Lett. B*, 428:241, 1998.

[14] F.A.Beck. *CRN(Strasbourg)-PN 84-41*, 1984.

[15] L.Bianchi *et al. Nucl. Inst. Methods in Phys. Res. A*, 276:509, 1989.

[16] F.Ajzenberg-Selove *et al. Nucl. Phys. A*, 490:1, 1988.

[17] *Cern Library Long Writup W5013*, 1994.